Influence of climate and land cover on river discharge in the North Fork Stillaguamish River

Jason E. Hall, Timothy J. Beechie, George R. Pess

Northwest Fisheries Science Center, NOAA Fisheries

Final Contract Report to:

Stillaguamish Tribe of Indians

Abstract

We analyzed trends in a wide range of flow and climate metrics using the Indicators of Hydrologic Alteration software. We then examined correlations between the flow metrics and potential drivers to ascertain whether climate trends, climate oscillations, or logging were the most likely drivers of temporal patterns in stream flows. We found increasing trends in peak flows (1-day, 3-day and 7-day average high flows), and that those trends are most likely driven by long-term climate trends, specifically increasing rainfall and decreasing snowfall. High flows increased steadily throughout the time period of analysis (1954-2011), whereas the proportion of immature forest land cover increased from 1954 to 1991 and declined from 1991 to 2011. Hence, land cover was not correlated with trends in high flow. Low flows (1-day, 3-day and 7-day average low flows) did not show a significant linear trend during the 1954-2011 time period. Rather, low flows increased during the first part of the study period and decreased during the second part. Low flows were correlated with total annual rainfall and snowfall, as well as land use and the climate oscillation metrics, suggesting that both decadal oscillations in climate and the timing of clearcutting may have influenced low flows, but it is not possible to discern which drivers are most important with our analysis. These results indicate that climate trends and oscillations are a likely cause of changes in both flood flows and low flows, although low flows may also have been influenced to some degree by land use.

Introduction

Recent trends in peak flows (both increasing and decreasing) have been documented throughout the world, and often those trends are attributed to climate change while the influence of land use is ignored or considered small (Hirsch and Ryberg, 2012; Collins, 2009). However, it is well known that land cover changes can influence peak flows through changes in tree cover, road density, or impervious surface area. Logging-related reductions in tree cover reduce interception of snow and rain, which can increase peak flows (Harr 1986, Jones 2000). Logging also decreases evapotranspiration which can increase annual water yield (Harr et al. 1975, Harr 1976, Hetherington 1982, Duncan 1986, Keppler and Ziemer 1990, Jones 2000). Increased road density effectively increases drainage density, which speeds the delivery of water to streams and increases peak flows (Harr et al. 1975, Jones and Grant 1996). Increased impervious area also speeds water delivery to streams by reducing infiltration into soils (Booth & Jackson 1997). The primary mechanisms by which climate trends can influence peak or low flows are (1) changes in precipitation driven by long-term climate change or by shorter term (decadal) climate cycles (McCabe and Wolock 2011), and (2) shifts from snow to rain as temperatures warm (Hisdal et al., 2007). Peak flow increases most commonly reflect increased storm size or intensity, whereas low flows are more likely to reflect changes in annual precipitation (either rain or snow). Shifts from snow to rain can also increase peak flows because flood flows driven by rain storms are generally much larger than those driven by snowmelt.

In this report we analyze potential causes of changes in peak and low flows in the Stillaguamish River basin, with the primary intent of evaluating whether or not land use practices might have caused increasing peak flows over the last few decades. We first summarize a range peak and low flow statistics using the Indicators of Hydrologic Alteration (IHA) software, and determine which flow parameters have shown increasing or decreasing trends over the past several decades. We also examine trends in logging rates and precipitation and snowfall, and use correlation analysis to identify potential climate and land use drivers that are most strongly related to flow trends in the Stillaguamish River basin. Finally, we use model selection to understand which mechanisms are likely the dominant drivers of observed trends in stream flow.

Methods

Discharge

Daily mean discharge data were obtained from USGS station 12167000 (available at http://waterdata.usgs.gov). This gage is located on the North Fork of the Stillaguamish River near Arlington, WA and is the only active gage with long-term daily discharge data available within the Stillaguamish River watershed (8/1/1928 – present). The gage has an

upstream drainage area of 679 km^2 and is located at river kilometer 10.4 at 48°15'42"North and 122°2'47"West. This gage does not capture discharge from the South Fork Stillaguamish River. Daily flow data was summarized using Indicators of Hydrologic Alteration software (IHA Version 7.7) to calculate 1-day, 3-day, 7-day, 30-day, and 90-day maximum and minimum flows, 7-day median maximum and minimum flow, and base flow index (7-day minimum flow/annual mean flow) by water year from 1929 to 2012. Days above 10,000 CFS by water year were also derived from daily flow data.

Local Climate

Precipitation and snowfall data were obtained from the National Climatic Data Center Global Historical Climatology Network (NCDC GHCN, available at http://www.ncdc.noaa.gov/). Local climate data with comparable temporal coverage to river discharge were limited to two stations within the Stillaguamish River watershed. In the lower watershed, local climate data were obtained from GHCN station 00450257 located in Arlington, WA at 48°12'0" North and 122°7'41" West at 30.5 meters elevation. Daily precipitation and snowfall data (recorded in tenths of mm) are available from 10/1/1928 to present at the Arlington station. Higher in the watershed, climate data were obtained from GHCN station 00451992 located in Darrington, WA at 48°15'36" North and 121°36'11" West at 167.6 meters elevation. Daily precipitation and snowfall data are available from 12/1/1911 to present at the Darrington station.

Total cumulative annual precipitation was derived by water year (October – September) from daily precipitation totals for each station. Total cumulative precipitation was not derived for water years with less than 350 days of record. Total cumulative annual snowfall was derived by water year (October – September) for the months of November through February from daily snowfall totals for each station. Total cumulative annual snowfall was not derived for water years with less than 100 days of daily records during this period (November – February). Antecedent precipitation accumulations were derived from the day of the 1-day maximum flow event and up to four days before the 1-day maximum flow event by water year using R statistical software (R Version 2.15.2).

Regional Climate

Monthly Pacific Decadal Oscillation (PDO) index data were obtained from the University of Washington (UW, available at http://jisao.washington.edu/pdo/PDO.latest) for water years 1929 to 2012. Monthly North Pacific Gyre Oscillation (NPGO) index data were obtained from California Current Ecosystem Long Term Ecological Research (CCE LTER, available at http://www.o3d.org/npgo/) for water years 1950 to 2012. Monthly Southern Oscillation Index (SOI) data were obtained from the National Atmospheric and Oceanic Administration (NOAA, available at http://www.pfeg.noaa.gov/products/PFEL/modeled/indices/NOIx/noix.html) for water years 1951 to 2012. Monthly coastal upwelling index (UWI) values from four stations

(48°North and 125°West, 51°North and 131°West, 54°North and 134°West, and 57°North and 137°West) were obtained for water years 1946 to 2012 from the National Atmospheric and Oceanic Administration (NOAA, available at http://www.pfeg.noaa.gov/). Summer (May – September) and winter (December – March) cumulative index values were derived from the monthly index values for PDO, NPGO, SOI, and UWI. Monthly averages of sea surface temperature (SST) were obtained from 12 coastal British Columbia lighthouse monitoring stations (Active Pass, Amphitrite Point, Bonilla Island, Chrome Island, Departure Bay, Egg Island, Entrance Island, Kains Island, Langara Island, McInnes Island, Pine Island, and Race Rocks) maintained by Fisheries and Oceans Canada (available at http://www.pac.dfo-mpo.gc.ca/science/oceans/data-donnees/lighthouses-phares/index-eng.htm). Station records begin in water year 1914 to 1970 (1943 average) by station and continue through water year 2012. Monthly SSTs from all 12 stations were used to derive average SST by water year.

Land Cover

Land cover data was developed by CORE GIS, LLC for the North Fork Stillaguamish River basin (CORE GIS 2012). Level 1 Landsat 5 TM imagery from the USGS was used to derive land cover classifications for five years (1987, 1991, 2001, 2006, and 2011). Land cover in 1954 was digitized from aerial photography. (We note here that a time series of road densities was not available, so we could not address the potential for roads to influence peak flows). Land cover was classified into the following land cover types and functional hydrological maturity groups:

Hydrologically mature land cover types

1. Mature evergreen forest: Hydrologically mature and contributes to large wood debris (LWD) which is likely to be in excess of 60 cm in diameter and 15.2 m in length. Overlay analysis with Forest Service stand age data defines this class as being at least 100 years old.
2. Medium evergreen forest: Hydrologically mature and does not contribute to LWD, but contributes to woody debris which are greater than 10 cm in diameter and 2.0 m in length. Overlay analysis with Forest Service stand age data defines this class as being 27 to 99 years old.
3. Deciduous stands: Hydrologically mature and in most cases does not contribute to LWD, but contributes to wood debris which are greater than 10 cm in diameter and 2.0 m in length.

Hydrologically immature land cover types

4. Shrubs and small trees: Hydrologically immature, but may provide small amounts of wood debris which are greater than 10 cm in diameter and 2.0 m in length; contains scrub/shrub, vegetated clearings, and industrial saplings.

5. Grass: Hydrologically immature, contains agricultural crops, grass, meadow, marsh, wetland, and recent clearcuts.
6. Bare ground: Hydrologically immature, consists of bare soil in agricultural, rural, and urban areas; also gravel pits and recent clearcuts.
7. Medium density development: Hydrologically immature, consists predominately of urban and suburban residential and commercial; contains roads, roofs, lawns, landscaping, and limited amounts of bare ground.
8. High density development: Hydrologically immature, consists of urban residential, commercial, and industrial; road, roof, parking lots, and sand/gravel bars.
9. Alpine rock and talus slopes: Hydrologically immature, consists predominately of high elevation exposed rock and talus slope.

Unclassified hydrologically mature land cover types

10. Open water: Lakes, large rivers, and reservoirs.
11. Unknown: Shadows and clouds.

The total area of hydrologically immature land cover by year was estimated using GIS (ArcMap V10.0). The proportional areas of land cover by functional hydrologically maturity were calculated for each year. Linear regressions between each sequential year pair were used to estimate the proportion of hydrologically immature land cover for each year from 1954 and 2012 (see Appendix A for table of values).

Relationships among flow, climate, and land cover

Temporal trends and relationships among flow, local climate, and regional climate metrics were analyzed with linear regressions using R statistical software (R Version 2.15.2). Predictive models for 1-day maximum and 1-day minimum flows were developed using an information theoretic approach to identify linear regression models with no collinear factors. The key principles behind this approach are that multiple models provide information about dependent variables and the best models are those that have strong predictive power but use fewer independent variables. The general strategy for this approach is to identify candidate models and test them using Akaike's Information Criterion (AIC), which scores models based on their ability to reduce uncertainty but penalizes by the number of variables in the model (Burnham and Anderson 2002). This approach differs greatly from inferential statistical analysis using stepwise regression by not focusing on null hypothesis testing (null hypotheses are usually poor models), p-values to falsify null hypotheses (arguably, there is no real difference between models with $p=0.055$ and $p=0.045$), and stepwise procedures optimizing based on R^2 and p-values. Stepwise models are highly sensitive to the order variables enter and often produce models with low predictive power. However, AIC scoring requires comparisons based on the same sample set and therefore reduces our sample size to years where all candidate metrics have available data. As a result, the AIC analysis is based on 19 years with complete data

between 1955 and 2006 for the maximum flow model and 38 years with complete data between 1954 and 2010 for the low flow model. Most data gaps are due to missing data or low quality data from local climate records.

Results

Temporal trends in discharge, climate, and land cover

Maximum 1-day, 3-day, and 7-day flows have a statistically significant ($p < 0.05$) increasing trend by water year, while 30-day and 90-day maximum flows have a moderately significant ($p < 0.1$) positive increasing trend over time (Table 1). The slope of the positive relationship decreases as the maximum flow period increases from 1-day to 90-day maximum flows (Table 1), with 1-day maximum flows having the strongest positive trend by water year (Figure 1). Both the number of days above the median 7-day maximum flow (8,569 CFS) and above 10,000 CFS have a statistically significant ($p < 0.05$) increasing trend by water year (Table 1, Figure 2). Of the minimum flow metrics, the base flow index (7-day minimum flow/annual mean flow) was the only metric that had a statistically significant ($p < 0.05$) temporal trend, with base flows decreasing over time (Table 1, Figure 3).

Of the local climate metrics evaluated, cumulative annual precipitation at Arlington and snowfall at Darrington were the only metrics that had statistically significant ($p < 0.05$) temporal trends (Table 1). Cumulative annual precipitation at Arlington shows a significant increasing trend over time (Table 1, Figure 4), while snowfall at Darrington has a significant decreasing trend over time (Table 1, Figure 5). Of the regional climate metrics evaluated, cumulative summer and winter NPGO, and average annual SST were the only regional climate metrics that showed statistically significant ($p < 0.05$) temporal trends (Table 1, Figure 6, Figure 7). All three metrics show statistically significant increasing trends over time (Table 1, Figure 6, Figure 7).

The proportion of immature land cover in the North Fork Stillaguamish River basin increased from a low of 18.7% in 1954 to a maximum of 35.6% in 1991 (Table 2, Figure 8). After this peak, the proportion of immature land cover decreased from 1991 to 24.7% in 2011 (Table 2, Figure 8). The spatial distribution of immature and mature land cover types are shown for each year in Figure 9.

Local Precipitation/Snowfall and Flow

Cumulative annual precipitation at both Arlington and Darrington were significantly related to many of the minimum flow metrics (Table 3). Total annual cumulative precipitation at Arlington was positively related to all minimum flow periods except the 1-day minimum flow (Table 3), while precipitation at Darrington was positively related to all minimum flow periods (e.g., 1-day through 90-day minimums). The slope of these positive

relationships increased with increasing period (e.g., 1-day verses 90-day minimum flow) (Table 3), with the strongest positive relationships occurring between 90-day minimum flows and cumulative annual precipitation at both stations (Figure 10). Both the number of days below the 7-day median low flow and base flow index were negatively related to Arlington precipitation, while the negative relationship between the number of days below the median 7-day low flow and Darrington precipitation was moderately significant (Table 3).

Cumulative annual precipitation at both Arlington and Darrington was also significantly related to many of the maximum flow metrics (Table 3), with maximum flows by all periods (1-day through 90-day) and the number of days above the median 7-day high flow and 10,000 CFS having significant positive relationships with precipitation at Arlington and Darrington (Table 3). In contrast to minimum flows, the slope of the relationship between precipitation and maximum flows decreased with period (e.g., 1-day verses 90-day maximum flow) (Table 3), with the strongest relationship being between 1-day maximum flows and cumulative annual precipitation at both stations (Figure 11). The number of days above the median 7-day maximum flow and 10,000 CFS was positively related to cumulative annual precipitation at both Arlington and Darrington (Table 3), with the strongest relationship being between cumulative annual precipitation and 7-day maximum flows (Figure 12).

Total cumulative snowfall at both Arlington and Darrington were negatively related to the number of days below the median 7-day low flow with moderate significance ($p < 0.1$) (Table 3). Snowfall at Darrington was positively related to minimum flows for all periods (1-day through 90-day), with the slope of this relationship increasing with period length (e.g., 1-day verses 90-day) (Table 3, Figure 13).

Maximum 1-day flood events were positively related to antecedent precipitation accumulation at Arlington and Darrington up to four days before the flow event. These relationships were statistically significant for all antecedent periods tested except for the precipitation accumulation for the day of the event at Arlington (Table 4). The strongest relationship between antecedent precipitation and 1-day maximum flows was observed for the 2-day accumulated precipitation at Darrington (i.e., precipitation on the day of the event plus precipitation the day before) (Table 4). Given that antecedent precipitation accumulations at Arlington and Darrington show statistically significant positive relationships (linear regression: $p < 0.05$), the antecedent precipitation accumulation at Darrington between the day of and the day before the 1-day maximum flow event was selected to develop models for flow.

Regional Climate and Flow

Minimum flows were negatively related to both the cumulative summer and winter PDO index, with the magnitude of this relationship increasing with period (e.g., 1-day

versus 90-day minimum flows) (Table 5). The number of days below the median 7-day low flow was also significantly related to the winter and summer PDO index, with the number of days having a positive relationship with the PDO index (Table 5). The cumulative winter PDO index was significantly related to all maximum flow metrics (Table 5), with the slope of the negative relationship decreasing with period length (e.g., 1-day verses 90-day maximum flow). The number of days above the median 7-day high flow and 10,000 CFS were positively related to the winter PDO index (Table 5).

Both the winter SOI and UWI index were related to minimum flows, although the relationship between the winter SOI and minimum flows was stronger for longer low flow periods (7-day to 90-day minimum flows) as compared to shorter periods (1-day to 30-day minimum flows) for the winter UWI index (Table 5). The magnitude (slope) of these positive relationships increased with period (e.g., 1-day verses 90-day period), although some relationships were only moderately significant ($p < 0.1$) (Table 5). The number of days below the median 7-day low flow was negatively related to both the winter SOI and UWI index (Table 5). Maximum flow metrics were not related to winter UWI or SOI index, with the exception of a moderately significant ($p < 0.1$) positive relationship between winter SOI and 90-day maximum flows (Table 5).

Average SST was significantly related to all low flow metrics, with the magnitude of this negative relationship increasing with increasing period (1-day verses 90-day low flow) (Table 5). The number of days below the median 7-day low flow was positively related to average SST, while the base flow index was negatively related to average SST (Table 5).

Regional Climate and Local Precipitation/Snowfall

Cumulative annual precipitation at Arlington was positively correlated with cumulative summer SOI (Table 6), while cumulative annual precipitation at Darrington was positively correlated with cumulative summer and winter NPGO (Table 6). Cumulative annual precipitation at Darrington also had a moderately statistically significant negative relationship with SST (Table 6). Annual cumulative snowfall at Arlington and Darrington was negatively correlated with SST and the cumulative summer PDO index (Table 6), while snowfall was positively related to cumulative winter SOI and UWI (Table 6).

Land Cover and Flow

The proportion of the basin with immature land cover was correlated with all of the minimum flow metrics (1-day, 3-day, 7-day, 30-day, and 90-day minimum flows and days below the median 7-day minimum flow and base flow index) (Table 7). The relationship between immature land cover and 1-day, 3-day, 7-day, 30-day, and 90-day minimum flows was negative, with the slope increasing with increasing period length (e.g., 1-day verses 90-day minimum flow) (Table 7, Figure 14). The number of days below the 7-day minimum

flow was positively related to immature land cover, while the base flow index was negatively related to immature land cover (Table 7).

In contrast to low flow, the relationship between immature land cover and maximum flow metrics (1-day, 3-day, 7-day, 30-day, and 90-day maximum flows and days above the median 7-day maximum flow and 10,000 CFS) were not statistically significant (Table 7). Of these high flow metrics, the positive relationship between immature land cover and 1-day max flow was only moderately significant (Table 7, Figure 15).

Flow Models

1-Day Max Flow Model

A subset of local climate (precipitation at Arlington and Darrington, and snowfall at Darrington) and regional climate (winter PDO) were considered to develop the 1-day maximum flow model. Land cover was not considered given that maximum flow was not correlated with land cover. Of these factors, the best model ($\Delta AIC < 2$ and best R^2) considering one, two, and three factor model combinations was a two factor model consisting of the antecedent precipitation accumulation at Darrington between the day of and the day before the 1-day maximum flow event and the total cumulative precipitation at Arlington (Table 8). This selected model was then regressed against the full period of record where antecedent precipitation accumulation at Darrington and the total cumulative precipitation at Arlington were available to produce the final model coefficients and fit statistics (Table 8). Predicted 1-day maximum flows relative to observed and the lower and upper 95% confidence intervals of the prediction are provided in Figure 16.

1-day Min Flow Model

A subset of local climate (snowfall at Darrington), regional climate (summer and winter PDO, winter UWI, and SST), and the proportion immature land cover were considered to develop the 1-day min flow model. Of these factors, the best model ($\Delta AIC < 2$ and best R^2) considering one, two, and three factor model combinations was a two factor model consisting of the cumulative annual snowfall at Darrington and the proportion of immature land cover (Table 8). This selected model was then regressed against the full period of record where cumulative annual snowfall at Darrington and the proportion of immature land cover were available to produce the final model coefficients and fit statistics (Table 9). Predicted 1-day minimum flows relative to observed and the lower and upper 95% confidence intervals of the prediction are provided in Figure 17.

Discussion

The results of this analysis suggest that the increasing trend in peak flows is most likely driven by long-term climate trends, specifically increasing rainfall and decreasing snowfall.

Land cover does not appear to be correlated with trends in high flow. High flows increased steadily throughout the time period of analysis (1954-2011), whereas the proportion of immature forest land cover increased from 1954 to 1991 and declined from 1991 to 2011. This result is consistent with a prior analysis of changes in recurrence intervals of peak flows in the Stillaguamish basin, which showed that a flow with a 10-20 yr recurrence interval prior to 1950 (about 24,500 cfs) had become a 1 to 2-yr event during the period 1972-1995 (Waples et al. 2008). Low flow volumes did not show a significant linear trend during the 1954-2011 time period. Rather, low flows tended to increase during the first part of the study period and decrease during the second part. This pattern is similar to temporal patterns in both the climate indicators and land use, suggesting that both decadal oscillation climate patterns and the timing of clearcutting may have influenced low flows.

Land use (percent immature forest) was not correlated with any of the high flow characteristics. This is perhaps not surprising as there is little evidence that increased water yield is accompanied by significantly higher peak flows in the absence of roads or snowmelt (Rothacher 1973). Moreover, even where rain-on-snow events can cause flooding, the biggest effect of timber harvest is on smaller peak flows with recurrence interval (RI) less than one year (i.e., lower than the bankfull event) (Harr 1976, Harr 1986, Ziemer 1998). Larger flows tend to be dominated by the rainfall component of the storm, and the snowmelt component has little influence on the flood size.

Where there is no snow component, flood peaks will increase if rainfall is more rapidly transferred to the stream via reduced interception or more rapid routing (Harr et al. 1975, Ziemer 1981, Jones and Grant 1996). Timber harvest reduces interception, which may increase the amount of water reaching the stream during small storms (Harr 1986, Jones 2000). However, during large storms, the canopy and soils are effectively saturated and interception has less influence on flood size. Therefore, reduced interception caused by timber harvest is unlikely to have a substantial effect on large floods. Overall, effects of timber harvest on peak flows are most pronounced in small basins (< a few km^2) and in relatively small floods (<1- or 2-year recurrence interval). Moreover, the percent immature forest in this basin varies from only 19% to 36%, which might possibly cause a 4% change in peak flow if there is no attenuation of peak flows at much larger scales (based the relationship between percent of basin harvested and peak flow in Grant et al. 2008) . Because a number of mechanisms attenuate site-scale peak flows at larger basin scales (e.g., tributary flows are out of phase, floodplain storage, etc.), the likely peak flow change at the scale of the North Fork Stillaguamish is likely less than 4%. Road drainage networks may also contribute to more rapid routing, but to date studies have not been able to document those effects in large basins (>~60 km^2, Grant et al. 2008).

Cumulative annual precipitation was strongly correlated with all of the high flow metrics (though snowfall was not). The annual 1- day maximum flow was also correlated with antecedent precipitation before the peak flow (1- to 5-day cumulative precipitation).

These correlations indicate that peak flow is most strongly related to changes in precipitation. There were also mixed results for the climate oscillation variables. Only the winter PDO was correlated with the high flows, but the other oscillation metrics (e.g., summer PDO, SOI, NPGO, SST) were correlated with either precipitation or snowfall. Together these results suggest that the decadal climate oscillations are not a primary driver of the trend in peak flows. Rather, the long-term increasing trend in precipitation (perhaps in combination with declining snowfall) is the most likely driver of increasing high flows in the North Fork Stillaguamish River basin. The model selection for the 1-day maximum flow found that a two-variable model with cumulative annual precipitation at Arlington and 2-day antecedent precipitation at Darrington was the best fit, supporting a conclusion that land use and climate oscillations were not strong drivers of the trend in flood flows.

Recent research into weather patterns that produce large rainstorms indicates that most large precipitation events in western Washington are associated with atmospheric rivers (which in the past have been commonly referred to as the "pineapple express") (Warner et al. 2012). These atmospheric rivers develop in the southwest Pacific Ocean and carry precipitable water to the PNW in relatively narrow bands (200—300 km wide). Notably, Warner et al. (2012) detected no temporal trends in the size of precipitation events across the west coast of the US in the last 60 years, and Neiman et al. (2011) found that most large floods in four western Washington Rivers were associated with atmospheric rivers in the past 30 years. This contrasts with our finding that both precipitation and 1-day average peak flows have an increasing trend over the past 80 years. It is not clear whether these contrasting results are due to differences in length of the period of record for each analysis, or whether temporal trends in the Stillaguamish are due to some factor other than atmospheric rivers influencing the precipitation trend.

While it seems clear that increasing precipitation is likely responsible for increasing peak flows in the Stillaguamish River, there is also the possibility that decreased attenuation of peak flows via decreased floodplain storage contributes to the trend. Significant channel straightening occurred between 1933 and 1955, but channel length has remained essentially constant since 1955 (Stillaguamish Tribe, unpublished data). The length of armored banks has increased steadily from 1933, but it does not appear that significant leveeing has occurred over that time frame. However, comparison of aerial photographs between 1933 and the present indicate that the channel is likely narrower and deeper in the past few decades, which may contribute to reduced overbank flooding and peak flow attenuation. This could contribute to increased peak flows at the gage, but flood magnitudes in the upper north Fork and tributaries would not be affected.

With respect to potential impacts to salmon populations, Grant et al. (2008) concluded that peak flows must have sufficient force to move bed-load material to affect a channel's physical structure, and that peak flow effects should therefore be confined to channels with

gradient is less than 2% and streambeds comprised of gravel or finer material. Notably, this area overlaps the majority of anadromous salmon habitats in most river basins (e.g., Lunetta et al. 1997, Burnett et al. 2007). However, there is no evidence that significant habitat changes occur at recurrence intervals of less than 5 years and a recent study of Chinook salmon in Skagit River basin showed that egg-to-migrant fry survival is significantly decreased at recurrence intervals of more than 5 to 6 years (Beamer et al. 2005). While the exact mechanism by which survival is reduced (scouring of redds, increased fines in the gravel, or decreased survival of emergent fry; Quinn 2005) remains unknown, the important fact is that peak flow increases caused by logging are only apparent for peak flows with recurrence intervals less than 5 years, while peak flows that affect salmon survival have only been documented at peak flows with recurrence intervals greater than 5 years.

In the single factor analyses examining correlations between low flows and climate, land use, or precipitation/snowfall variables, there were strong correlations with all of the independent variable categories. The proportion of immature forest was one of the strongest correlates, and it was correlated with every low flow metric examined (1-, 3-, 7-, 30-, and 90-day minima, base flow, and number of days below the median 7-day minimum). The likely mechanism underlying this correlation is an increase in total water yield due to reduced evapotranspiration (Harr et al. 1975, Harr 1976, Hetherington 1982, Duncan 1986, Keppler and Ziemer 1990, Jones 2000). Effects on water yield appear to increase with increasing percent of basin harvested, and there is no clear threshold above which the impact is significant. However, one study suggests the effect becomes detectable when more than 25% of the basin is harvested (Stednick 1996). Low flows increase (especially in summer) because more water is available for runoff over the year (Hetherington 1982), and are most evident in the first 10 years after harvest (Hicks et al. 1991, Jones 2000). In the Stillaguamish River basin, the highest percent immature forest was 35% and the lowest 19%, suggesting that the proportion of basin harvested was high enough to increase low flow compared to an unharvested basin throughout much of the analysis period. However, the percent of basin harvested varied by only 16% during the analysis period, suggesting that changes in low flow due to timber harvest may not be statistically detectable

The climate variability indicators were also correlated primarily with low flows. Both annual precipitation and annual snowfall were positively correlated with most of the low flow indicators, suggesting that years with more water and or snow tended to have higher low flows. Annual snowfall was also correlated with the PDO index, suggesting that climate oscillations may be a partial driver of the temporal pattern of low flows. However, it is notable that all of the potential driving variables (land use, local rainfall/snowfall, and the regional climate indicators) have approximately the same temporal pattern, so it is not possible to definitively ascribe changes in low flows to any one variable or combination of variables. Moreover, the best model for the 1-day minimum flow was a two-variable model

with proportion of immature land cover and total annual snowfall at Darrington (which was correlated with several climate oscillation indices), suggesting that land use and decadal climate patterns are similarly important correlates with low flows.

Literature Cited

Beamer, E.M., and G. Pess. 1999. Effects of peak flows on Chinook (*Oncorhynchus tshawytscha*) spawning success in two Puget Sound River basins. *In* Watershed management to protect declining species. *Edited by* R. Sakrison and P. Sturtevant. American Water Resources Association. pp. 67-70

Booth, D.B. & Jackson, C.R. (1997) Urbanization of aquatic systems – degradation thresholds, stormwater detention, and the limits of mitigation. *Water Resources Bulletin* **33**, 1077–1090.

Burnett, K.M, G.H. Reeves, D.J. Miller, S. Clarke, K. Vance-Borland, and K. Christiansen. 2007. Distribution of salmon-habitat potential relative to landscape characteristics and implications for conservation. Ecol. Appl. 17(1): 66-80.

Burnham, K. P., and D. R. Anderson 2002. Model selection and multimodel inference: a practical information-theoretic approach. Springer-Verlag, New York.

Collins, M. J., 2009. Evidence for changing flood risk in New England since the late 20th century. Journal of the American Water Resources Association 45, 279-290. doi:10.1111/j.1752-1688.2008.00277.x

CORE GIS. 2012. Stillaguamish River Watershed 1954 Landcover. Technical Report prepared for Stillaguamish Tribe of Indians.

Duncan, S.H. 1986. Peak discharge during thirty years of sustained yield timber management in two fifth order watersheds in Washington state. Northwest Science 60(4):258-264.

Grant, G.E., S.L. Lewis, F.J. Swanson, J.H. Cissel, J.J. McDonnell. 2008. Effects of forest practices on peak flows and consequent channel response: a state-of-science report for western Oregon and Washington. Gen. Tech. Rep. PNW-GTR-760. U.S. Dept. of Ag., Forest Service, Pacific Northwest Research Station, Portland, OR. 76 p.

Harr, R. D., W. C. Harper, J. T. Krygier, and F. S. Hsieh. 1975. Changes in storm hydrographs after road building and clear-cutting in the Oregon Coast Range. Water Resources Research 11(3):436-444.

Harr, R.D. 1976. Forest practices and streamflow in western Oregon. USDA Forest Service Technical report PNW-GTR-49. (In: Adams and Ringer 1994).

Harr, R.D. 1986. Effects of clearcutting on rain-on-snow runoff in western Oregon: A new look at old study. Water Res. Bull. 22(7):1095-1100.

Hetherington, E.D. 1982. A first look at logging effects on the hydrologic regime of Carnation Creek Experimental Watershed. pp 36-44. In: Hartman, G. (ed). Proceedings of the Carnation Creek Workshop, a 10 year review. Malaspina College, Nanaimo, B.C.

404 pp. (In Adams and Ringer 1994).

Hicks, B. J., R. L. Beschta and R. D. Harr. 1991. Long-term changes in streamflow following logging in western Oregon and associated fisheries implications. Water Res. Bull. 27(2):217-226.

Hirsch, R.M., Ryberg, K.R., 2012. Has the magnitude of floods across the USA changed with global CO_2 levels? Hydrological Sciences Journal 57, 1-9.

Hisdal, H., Holmqvist, E., J´onsd´ottir, J.F., J´onsson, P., J¨arvet, A., Lindstr¨om, G., Kolcova, T., Kriauciuniene, J., Kuusisto, E., Lizuma, L., Meilutyte-Barauskiene, D., Reihan, A., Roald, L.A., 2007. Climate change signals in streamflow data in the Nordic and Baltic region. In , Heinonen, M. (Ed), Proceedings of the Third International Conference on Climate and Water, 3–6 September 2007, SYKE, Helsinki, Finland, pp. 182–187.

Jones, J.A. 2000. Hydrologic processes and peak discharge response to forest removal, regrowth, and roads in 10 small experimental basins, western Cascades, Oregon. Water Ressources Research, 36(9):2621-2642.

Jones, J.A. and G.E. Grant. 1996. Peak flow response to clear-cutting and roads in small and large basins, western Cascades, Oregon. Water Res. Bull 52(4):459-474.

Keppler, E.T. and R.R. Ziemer. 1990. Logging effects of streamflow: Water yield and summer low flows at Caspar Creek in Northwestern California. Water Res. Bull. 26(7):1669-1679. (In Adams and Ringer 1994).

Lunetta, R.S., B.L. Cosentino, D.R. Montgomery, E.M. Beamer, and T.J. Beechie. 1997. GIS-Based evaluation of salmon habitat in the Pacific Northwest. Photogrammetric Engineering and Remote Sensing 63: 1219-1229.

McCabe, G.J., Wolock, D.M., 2011. Independent effects of temperature and precipitation on modeled runoff in the conterminous United States. Water Resources Research 47, n/a–n/a. doi:10.1029/2011WR010630

Neiman, Paul J., Lawrence J. Schick, F. Martin Ralph, Mimi Hughes, Gary A. Wick, 2011: Flooding in Western Washington: The Connection to Atmospheric Rivers*. *J. Hydrometeor*, **12**, 1337–1358. doi: http://dx.doi.org/10.1175/2011JHM1358.1

Quinn, T.P. 2005. The behavior and ecology of pacific salmon and trout. University of Washington Press, Seattle, Washington.

Rothacher, J. 1973. Does harvest in west slope Douglas-fir increase peak flow in small forest streams? USDA Forest Service Res. Paper PNW-163. Portland.

Stednick, J.D. 1996. Monitoring the effects of timber harvest on annual water yield. Journal of Hydrology 176:79-95.

Waples, R. S., G. R. Pess, and T. Beechie. 2008. Evolutionary history of Pacific salmon in dynamic environments. Evolutionary Applications 1:189-206.

Warner, Michael D., Clifford F. Mass, Eric P. Salathé, 2012: Wintertime Extreme Precipitation Events along the Pacific Northwest Coast: Climatology and Synoptic Evolution. *Mon. Wea. Rev.*, **140**, 2021–2043.

doi: http://dx.doi.org/10.1175/MWR-D-11-00197.1

Ziemer, R. R. 1981. Storm flow response to road building and partial cutting in small streams of Northern California. Water Res. Bull. 17(4):907-917 (In Adams and Ringer 1994.

Ziemer, R. 1998. Flooding and stormflows. USDA Forest Service Gen. Tech. Rep., PSW-GTR-168, p. 15-24.

Table 1: Flow, local climate, and regional climate metrics with statistically significant ($p < 0.05$ and $p < 0.1$*) temporal trends by water year. Linear regression statistics for the intercept, slope, R^2, and p-value are provided for each metric.

Metric Group	Dependent	Intercept	Slope	R^2	P
Flow	Base Flow	0.846	-0.0004	0.055	0.0313
	1-day max	-206940.3	114.2	0.185	<0.0001
	3-day max	-103884.5	59.0	0.098	0.0038
	7-day max	-45602.98	27.49	0.057	0.0284
	30-day max	-15613	10.290	0.037	0.0777*
	90-day max	-8810.935	6.1840	0.041	0.0656*
	Days above median 7-day max	-80.268	0.0441	0.065	0.0195
	Days above 10,000 CFS	-77.041	0.0414	0.085	0.0070
Local Climate	Annual Cumulative Precipitation at Arlington (tenth mm)	-31438	21.87	0.073	0.0434
	Annual Cumulative Snow at Darrington (tenth mm)	21499	-10.503	0.127	0.0065
Regional Climate	NPGO Summer (Sum May-Sep)	-202.7	0.1027	0.142	0.0023
	NPGO Winter (Sum Dec-Mar)	-146.143	0.074	0.103	0.0102
	SST (Water Year Average)	-1.639	0.0059	0.091	0.0053

Table 2: Proportion of North Fork Stillaguamish watershed by functional hydrological land cover groups for each available year.

Hydrological Group	Land Cover Class	1954	1987	1991	2001	2006	2011
Mature	Mature evergreen forest	NA	0.260	0.301	0.307	0.320	0.356
	Medium evergreen forest	NA	0.319	0.249	0.256	0.283	0.303
	Deciduous stands	NA	0.102	0.095	0.098	0.095	0.094
Mature	**Total**	**0.813**	**0.680**	**0.644**	**0.661**	**0.697**	**0.753**
Immature	Shrub / small trees	NA	0.242	0.252	0.223	0.204	0.162
	Grass	0.069	0.015	0.035	0.046	0.045	0.043
	Bare ground	0.076	0.026	0.013	0.025	0.014	0.016
	Medium density development	0.000	0.010	0.010	0.017	0.014	0.009
	High density development	NA	0.001	0.001	0.000	0.002	0.001
	Alpine rock / talus slope	0.042	0.027	0.044	0.027	0.023	0.017
Immature	**Total**	**0.187**	**0.320**	**0.356**	**0.339**	**0.303**	**0.247**

Table 3: Local climate metrics with statistically significant ($p<0.05$ and $p<0.1$*) relationships with low and high flow metrics. Linear regression statistics for the intercept, slope, R^2, and p-value are provided.

Metric	Dependent	Intercept	Slope	R^2	P
Annual Cumulative Precipitation at Arlington (tenth mm)	3-day min	118.200	0.0096	0.078	0.0371
	7-day min	88.334	0.0137	0.119	0.0093
	30-day min	-9.421	0.0288	0.159	0.0023
	90-day min	-270.008	0.0743	0.328	<0.0001
	Days below median 7-day min	57.925	-0.0038	0.166	0.0018
	Base Flow	0.207	<-0.0001	0.096	0.0199
	1-day max	-6645.02	2.0952	0.351	<0.0001
	3-day max	-6987.21	1.6241	0.474	<0.0001
	7-day max	-2492.99	0.9270	0.384	<0.0001
	30-day max	-1147.00	0.4897	0.443	<0.0001
	90-day max	-538.788	0.3321	0.598	<0.0001
	Days above median 7-day max	-12.670	0.0016	0.454	<0.0001
	Days above 10,000 CFS	-11.040	0.0013	0.430	<0.0001
Annual Cumulative Precipitation at Darrington (tenth mm)	1-day min	38.744	0.0097	0.192	0.0467
	3-day min	44.090	0.0096	0.188	0.0493
	7-day min	63.907	0.0095	0.170	0.0633*
	30-day min	-86.488	0.0212	0.201	0.0418
	90-day min	-291.463	0.0454	0.308	0.0090
	Days below median 7-day min	53.725	-0.0020	0.150	0.0826*
	1-day max	-5609.86	1.0859	0.352	0.0046
	3-day max	-1714.00	0.6432	0.310	0.0087
	7-day max	521.622	0.3658	0.287	0.0124
	30-day max	348.918	0.2005	0.480	0.0005
	90-day max	268.758	0.1480	0.624	<0.0001
	Days above median 7-day max	-4.933	0.0005	0.276	0.0144
	Days above 10,000 CFS	-4.094	0.0004	0.239	0.0246
Annual Cumulative Snowfall at Arlington (tenth mm)	Days below median 7-day min	18.521	-0.0249	0.082	0.0811*
Annual Cumulative Snowfall at Darrington (tenth mm)	1-day min	206.675	0.0337	0.127	0.0066
	3-day min	217.140	0.0316	0.103	0.0148
	7-day min	234.010	0.0322	0.087	0.0260
	30-day min	303.188	0.0534	0.076	0.0384
	90-day min	504.419	0.1540	0.169	0.0015
	Days below median 7-day min	18.263	-0.0063	0.067	0.0525*

Table 4: Linear regression statistics for antecedent precipitation accumulation on the day of the1-day maximum flow event (Day 0) and up to four days before the peak flow event (day-4 – 0) with the 1-day maximum flows by water year.

Station	Precipitation Range	Slope	R^2	P
Darrington	Day 0	8.615	0.182	0.00032
	Day -1 - 0	7.629	0.240	0.00007
	Day -2 - 0	6.137	0.195	0.00074
	Day -3 - 0	4.892	0.158	0.00383
	Day -4 - 0	3.616	0.145	0.00703
Arlington	Day 0	8.588	0.032	0.12250
	Day -1 - 0	12.404	0.129	0.00142
	Day -2 - 0	10.048	0.112	0.00336
	Day -3 - 0	9.806	0.125	0.00190
	Day -4 - 0	9.893	0.149	0.00068

Table 5: Regional climate metrics with statistically significant ($p < 0.05$ and $p < 0.1$*) relationships with low and high flow metrics. Linear regression statistics for the intercept, slope, R^2, and p-value are provided.

Metric	Dependent	Intercept	Slope	R^2	P
PDO Summer	1-day min	232.992	-4.3910	0.098	0.0037
	3-day min	242.334	-4.7560	0.095	0.0043
	7-day min	257.973	-5.0860	0.092	0.0049
	30-day min	338.881	-8.8260	0.104	0.0028
	90-day min	614.125	-17.1420	0.115	0.0016
	Days below median 7-day min	13.494	1.2000	0.108	0.0023
PDO Winter	1-day min	230.993	-6.1590	0.130	0.0008
	3-day min	240.244	-6.2720	0.111	0.0019
	7-day min	255.615	-7.3630	0.130	0.0008
	30-day min	334.689	-13.3100	0.159	0.0002
	90-day min	606.180	-24.8200	0.162	0.0001
	Days below median 7-day min	14.074	1.8649	0.174	0.0001
PDO Winter	1-day max	17944.200	-315.4000	0.038	0.0765*
	3-day max	12313.400	-283.4000	0.061	0.0241
	7-day max	8536.560	-142.8700	0.041	0.0632*
	30-day max	4649.140	-98.0200	0.091	0.0052
	90-day max	3362.360	-64.8500	0.120	0.0012
	Days above median 7-day max	6.476	-0.3223	0.093	0.0048
	Days above 10,000 CFS	4.496	-0.2136	0.061	0.0237
SOI Winter	7-day min	259.379	4.5050	0.047	0.0897*
	30-day min	344.523	7.7860	0.049	0.0842*
	90-day min	616.882	15.4700	0.061	0.0537*
	Days below median 7-day min	12.912	-1.4918	0.146	0.0022
	90-day max	3465.430	44.0700	0.055	0.0674*
UWI Winter	1-day min	282.472	0.1211	0.049	0.0718*
	3-day min	299.002	0.1393	0.053	0.0602*
	7-day min	318.781	0.1506	0.052	0.0637*
	30-day min	447.947	0.2734	0.065	0.0374
	Days below median 7-day min	-0.469	-0.0342	0.085	0.0165
SST	1-day min	798.560	-56.1700	0.158	0.0002
	3-day min	830.530	-58.4200	0.141	0.0006
	7-day min	939.260	-67.6800	0.160	0.0002
	30-day min	1446.360	-109.9600	0.159	0.0002
	90-day min	3085.600	-245.7500	0.233	<0.0001
	Days below median 7-day min	-160.321	17.2260	0.256	<0.0001
	Base Flow	0.312	-0.0174	0.050	0.0406

Table 6: Relationships among regional and local climate metrics with statistically significant ($p < 0.05$ and $p < 0.1$*) relationships. Linear regression statistics for the intercept, slope, R^2, and p-value are provided.

Local Climate Dependent	Regional Climate Metric	Intercept	Slope	R^2	P
Arlington Precip	SOI Summer	11768.200	192.5300	0.138	0.0102
Darrington Precip	NPGO Summer	20298.200	494.9000	0.493	0.0236
	NPGO Winter	20653.000	771.7000	0.581	0.0104
	SST	48234.000	-2833.0000	0.147	0.0862*
Arlington Snow	PDO Summer	150.716	-15.2630	0.126	0.0287
	SOI Winter	134.938	13.3880	0.083	0.0934*
	UWI Winter	322.074	0.4763	0.121	0.0379
	SST	2064.070	-189.3600	0.213	0.0035
Darrington Snow	PDO Summer	822.060	-47.5500	0.105	0.0139
	SOI Winter	714.780	62.9400	0.152	0.0129
	UWI Winter	1522.273	2.0950	0.153	0.0096
	SST	11104.000	-1024.0000	0.511	<0.0001

Table 7: Linear regressions for flow and land cover (proportion immature land cover). Bold values indicate statistically significant linear regressions at $p < 0.05$.

Dependent	Intercept	Slope	R^2	P
1-day min	462.5	-789.13	0.302	**0.0000**
7-day min	452.0	-722.96	0.241	**0.0001**
3-day min	492.5	-807.90	0.242	**0.0001**
30-day min	658.2	-1081.17	0.149	**0.0025**
90-day min	1149.	-1819.8	0.134	**0.0043**
Days below median 7-day min	-26.52	135.02	0.194	**0.0005**
Base Flow	0.211	-0.2684	0.127	**0.0057**
1-day max	12002	26494	0.046	0.1035
3-day max	9770	12052	0.020	0.2874
7-day max	8152	3050	0.003	0.6708
30-day max	4819.4	210.8	0.000	0.9508
90-day max	3701.1	-690.8	0.002	0.7208
Days above median 7-day max	4.722	9.65	0.015	0.3616
Days above 10,000 CFS	2.449	10.13	0.022	0.2601

Table 8: Linear regression statistics for the selected two-factor 1-Day maximum flow model. Darrington antecedent precipitation includes precipitation on the day of and the day before the flow event.

Coefficient	Estimate	Std. Error	t-value	p-value
Intercept	-7312.191	5618.388	-1.301	0.202
Arlington Precipitation	1.734	0.487	3.557	0.001
Darrington Antecedent Precipitation	5.323	1.934	2.753	0.009
Residual standard error: 5155 on 35 degrees of freedom, Multiple R-squared: 0.426, Adjusted R-squared: 0.3932, F-statistic: 12.99 on 2 and 35 DF, p-value < 0.001.				

Table 9: Linear regression statistics for the selected 1-Day minimum flow model.

Coefficient	Estimate	Std. Error	t-value	p-value
Intercept	414.55	61.62	6.727	<0.001
Proportion Immature Land Cover	-694.92	198.19	-3.506	0.001
Annual Darrington Snowfall	0.037	0.015	2.523	0.016
Residual standard error: 56.15 on 35 degrees of freedom, Multiple R-squared: 0.459, Adjusted R-squared: 0.428, F-statistic: 14.85 on 2 and 35 DF, p-value < 0.001.				

Figure 1: 1-day maximum flow by water year, with linear regression trend line.

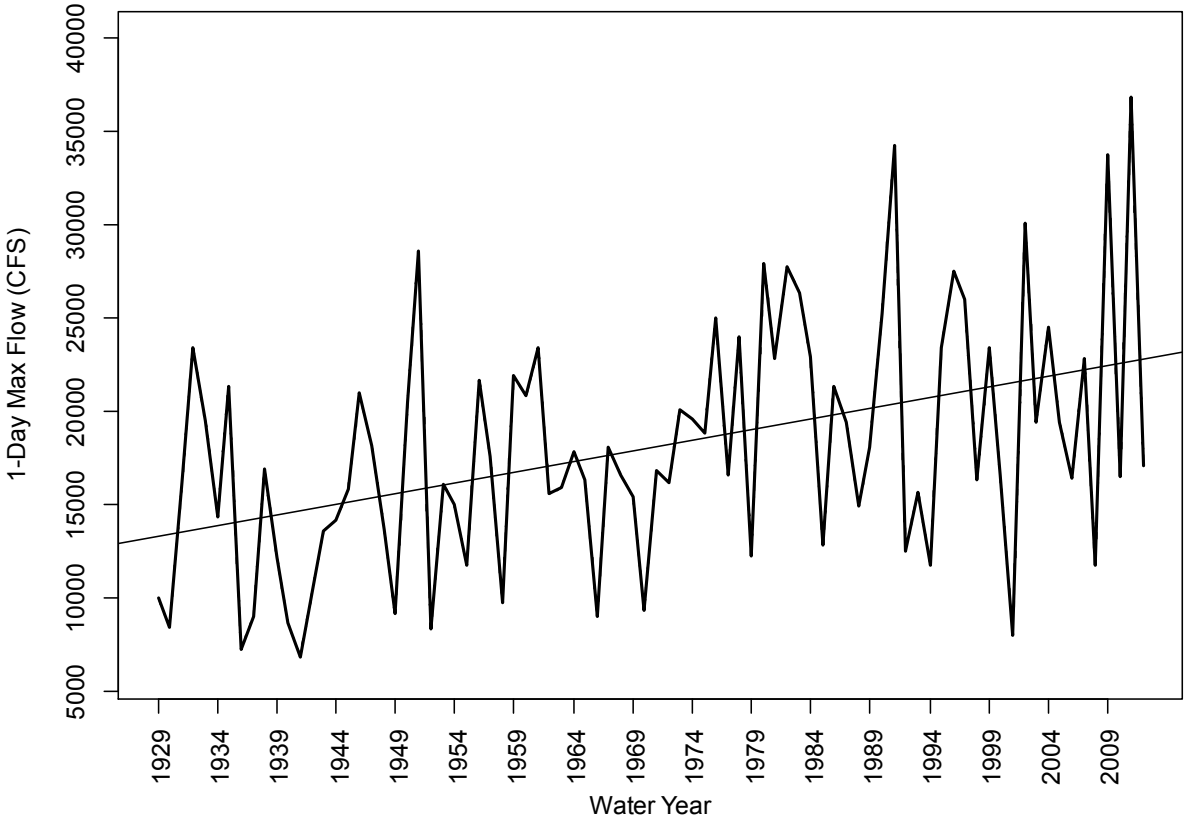

Figure 2: Days above 7-day median high flow (solid line) and days above 10,000 CFS (dashed line) by water year, with linear regression trend lines.

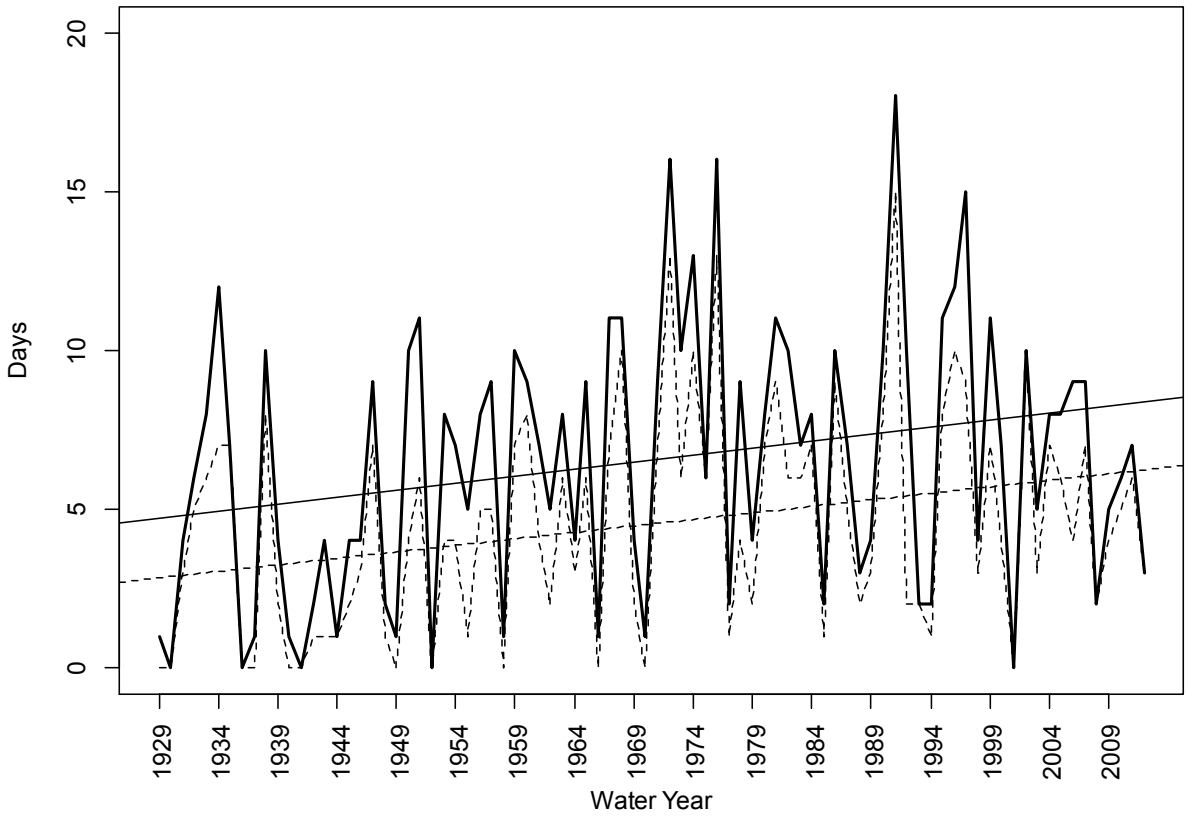

Figure 3: Base flow index (7-day minimum flow/annual mean flow) by water year, with linear regression trend lines.

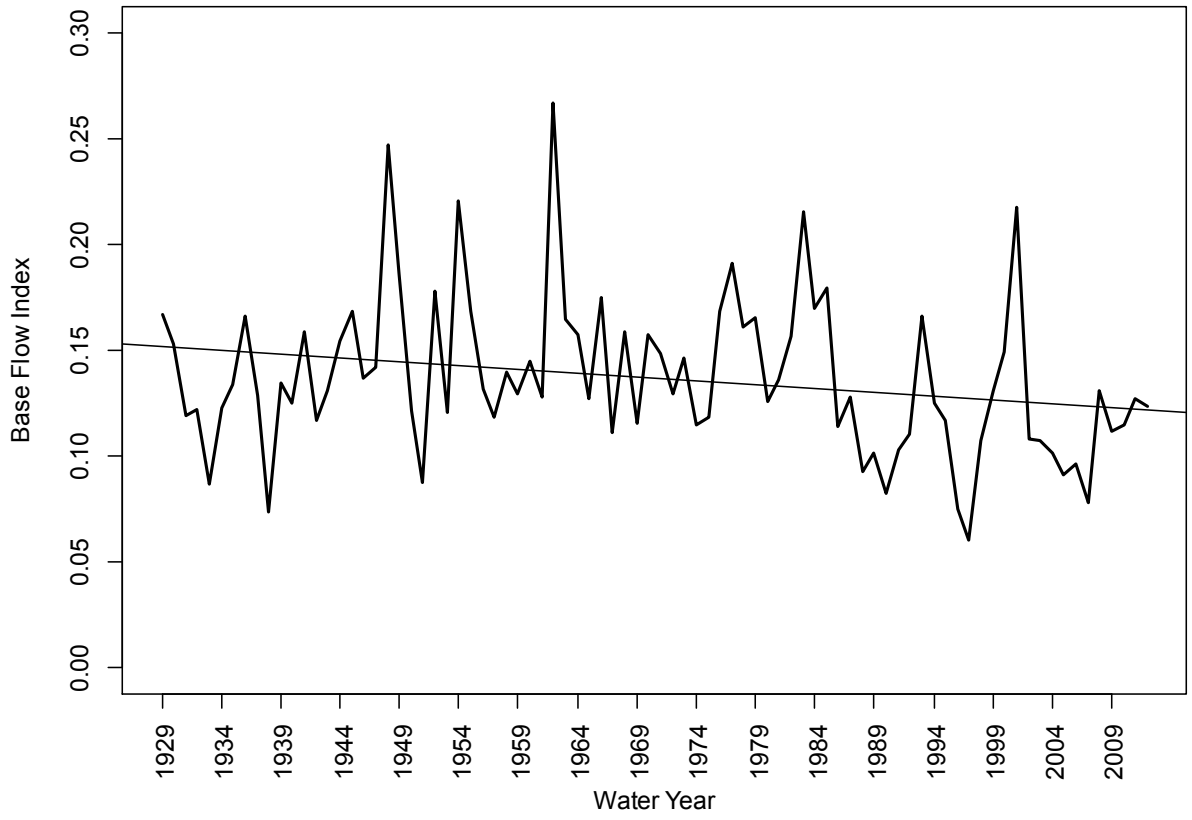

Figure 4: Total annual precipitation at Arlington, WA by water year, with linear regression trend line.

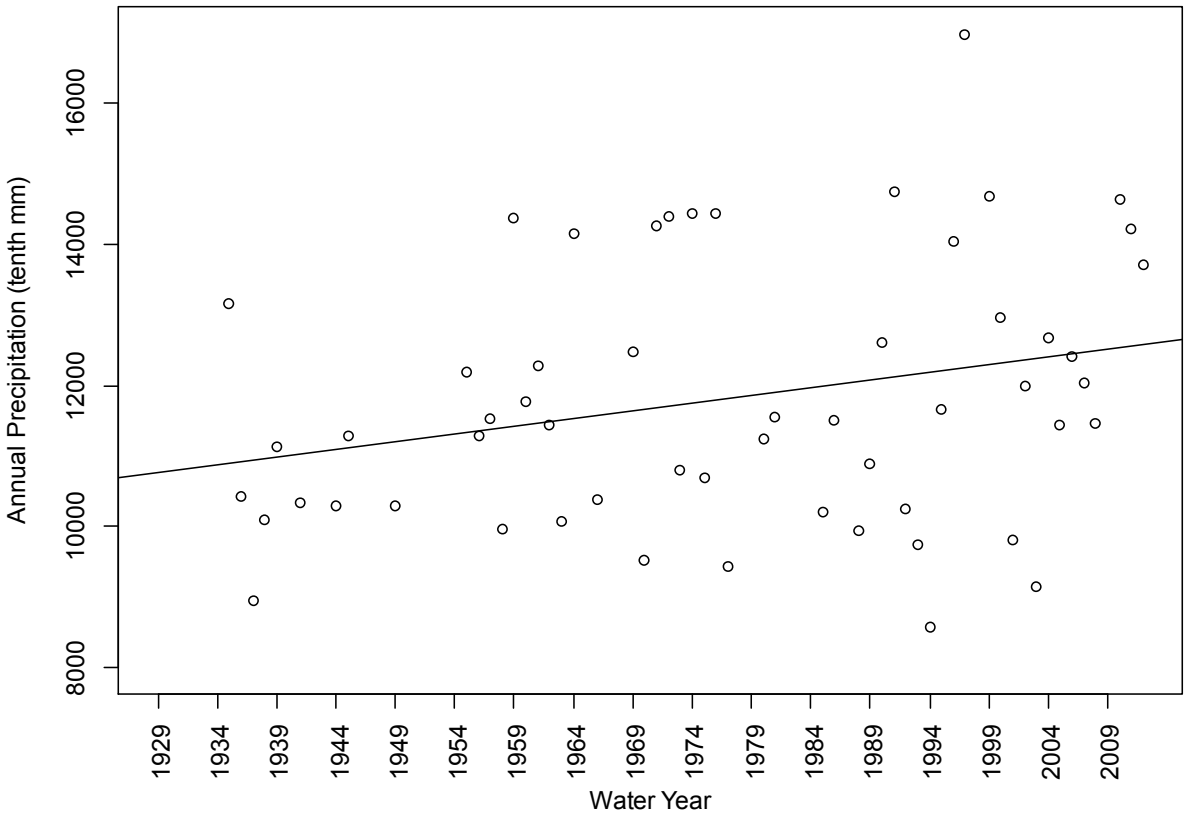

Figure 5: Total annual snowfall at Darrington, WA by water year, with linear regression trend line.

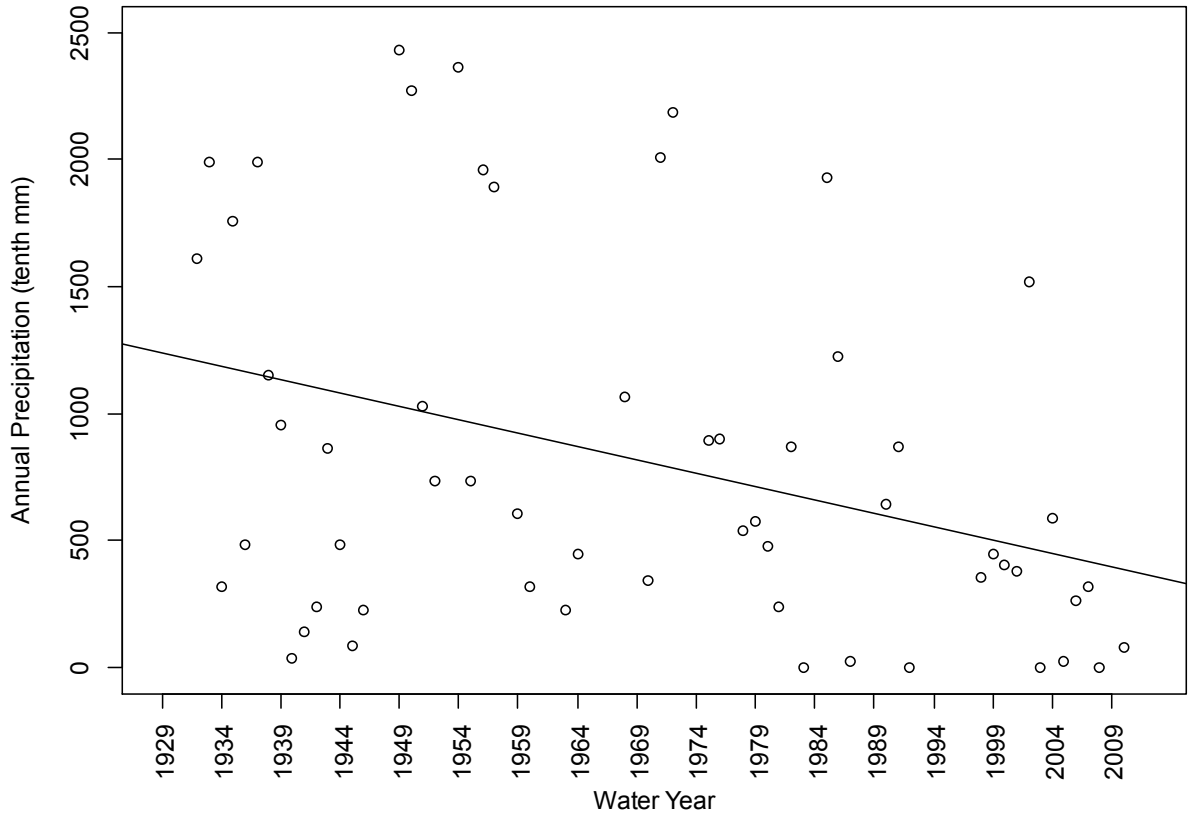

Figure 6: Cumulative summer (solid line) and winter (dashed line) NPGO Index by water year, with linear regression trend lines.

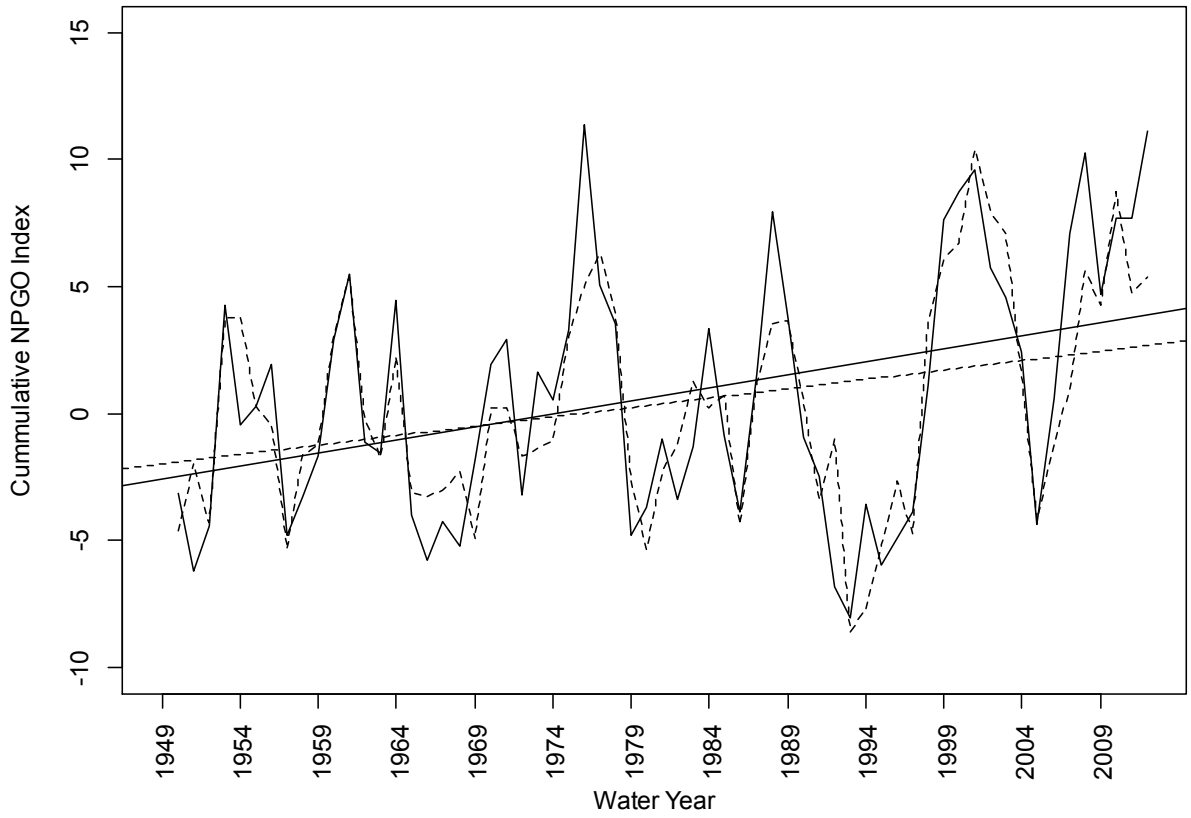

Figure 7: Average Sea Surface Temperature (SST) by water year with linear regression trend line.

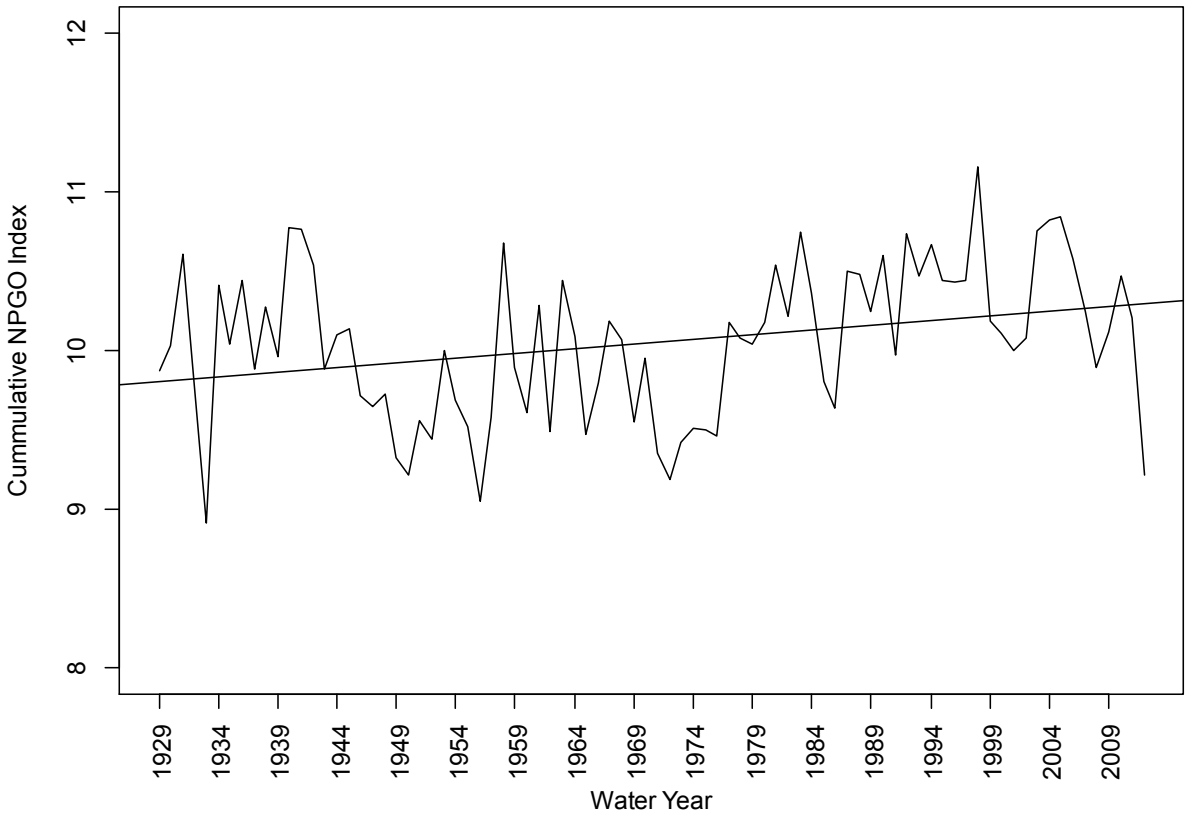

Figure 8: Proportion hydrologically mature and immature land cover classification by water year based on land cover classifications from water years 1954, 1987, 1991, 2001, 2006, and 2011.

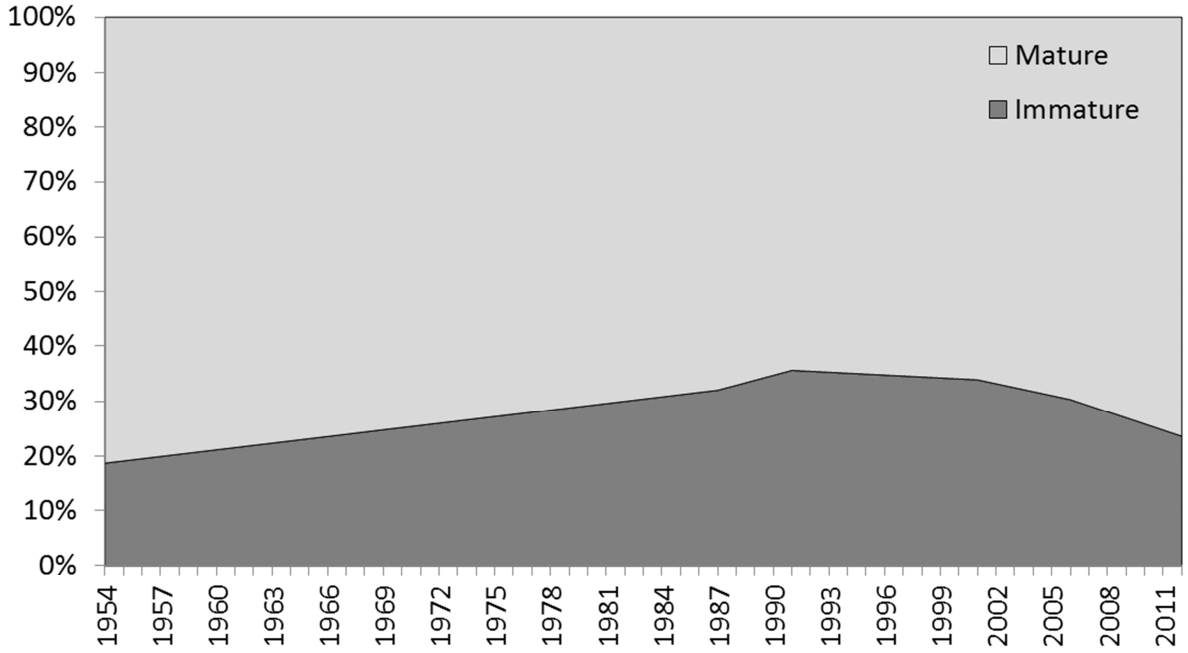

Figure 9: Immature and mature land cover distribution within the North Fork Stillaguamish Basin from 1954-2011.

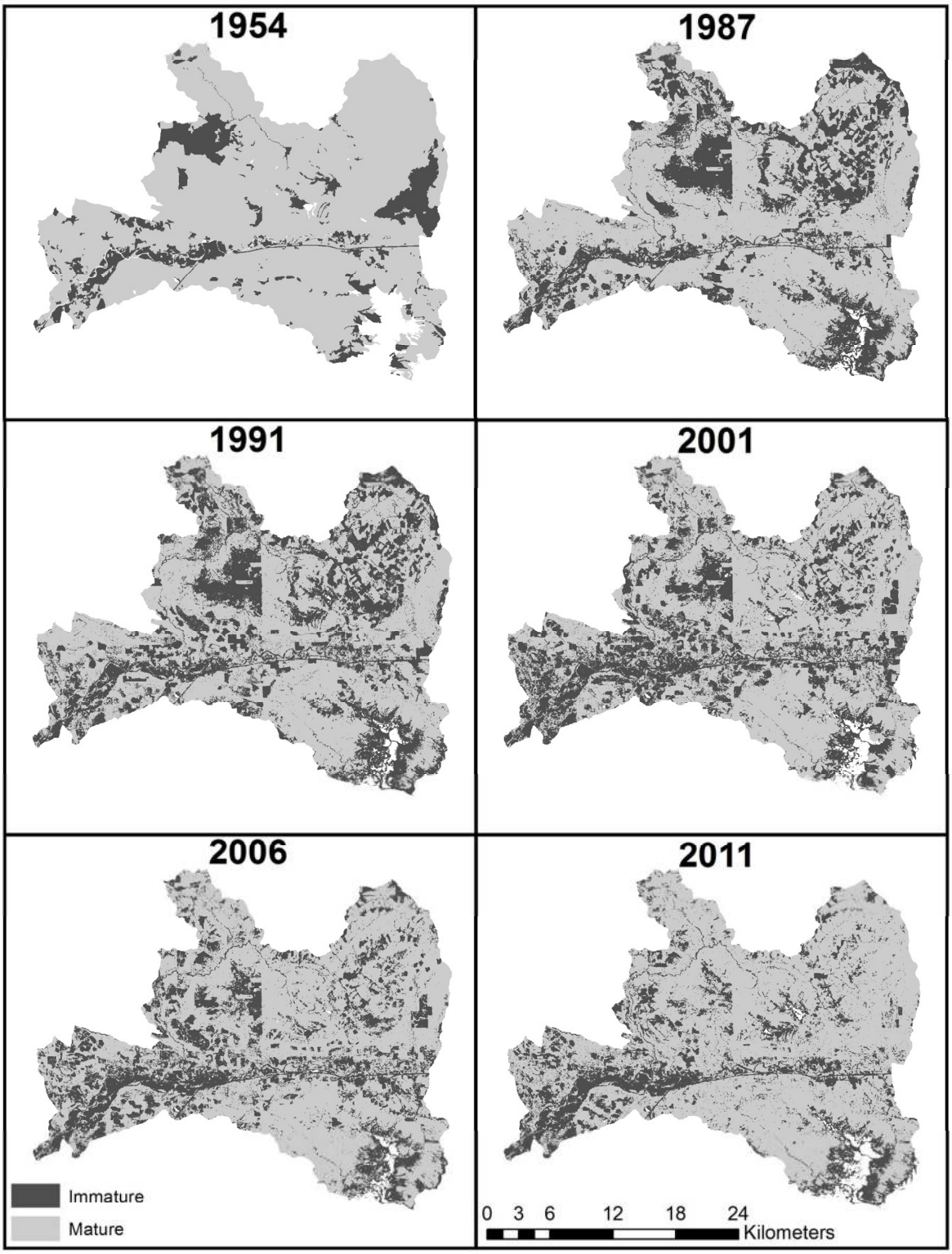

Figure 10: Cumulative annual precipitation at Arlington, WA (open circles) and Darrington, WA (solid circles) and 90-day minimum flows with linear regression trend lines.

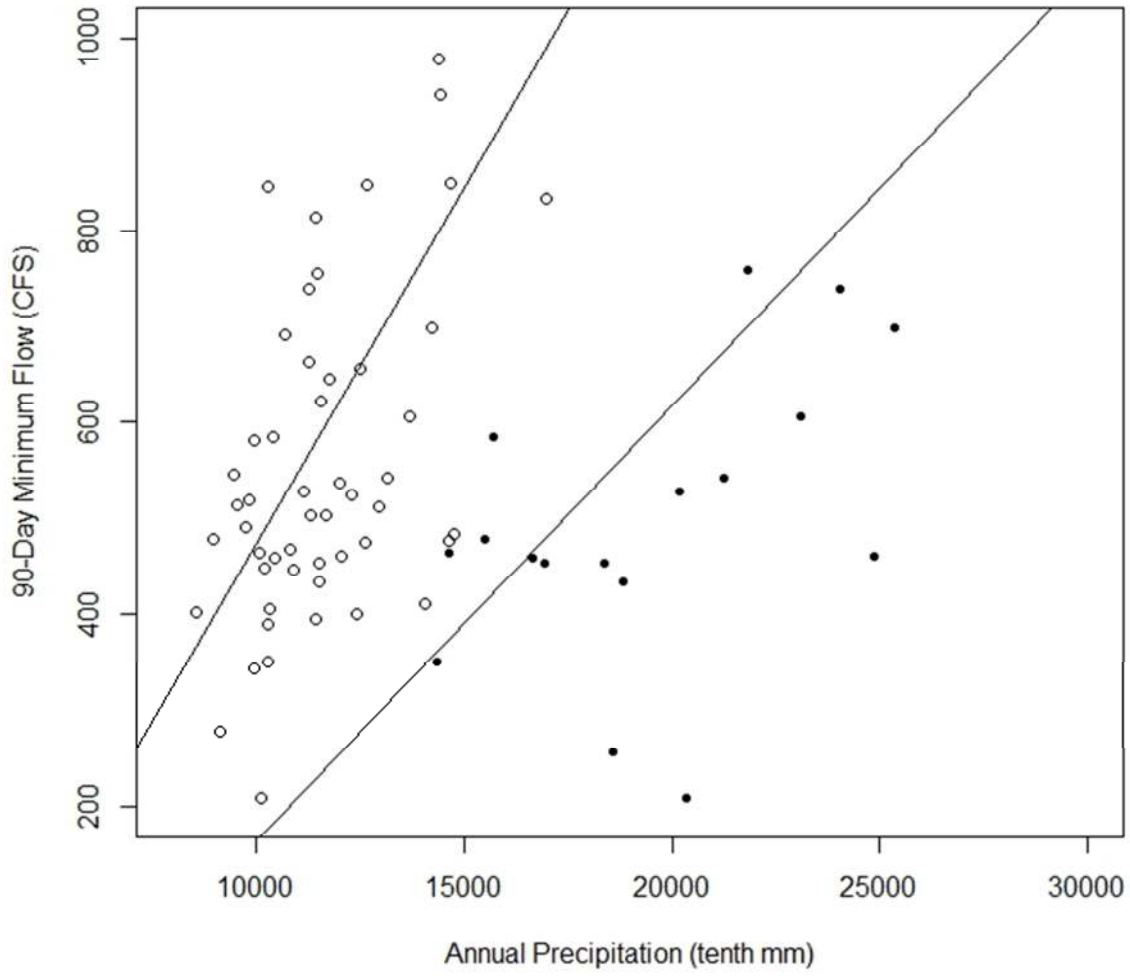

Figure 11: Cumulative annual precipitation at Arlington, WA (open circles) and Darrington, WA (solid circles) and 1-day maximum flows with linear regression trend lines.

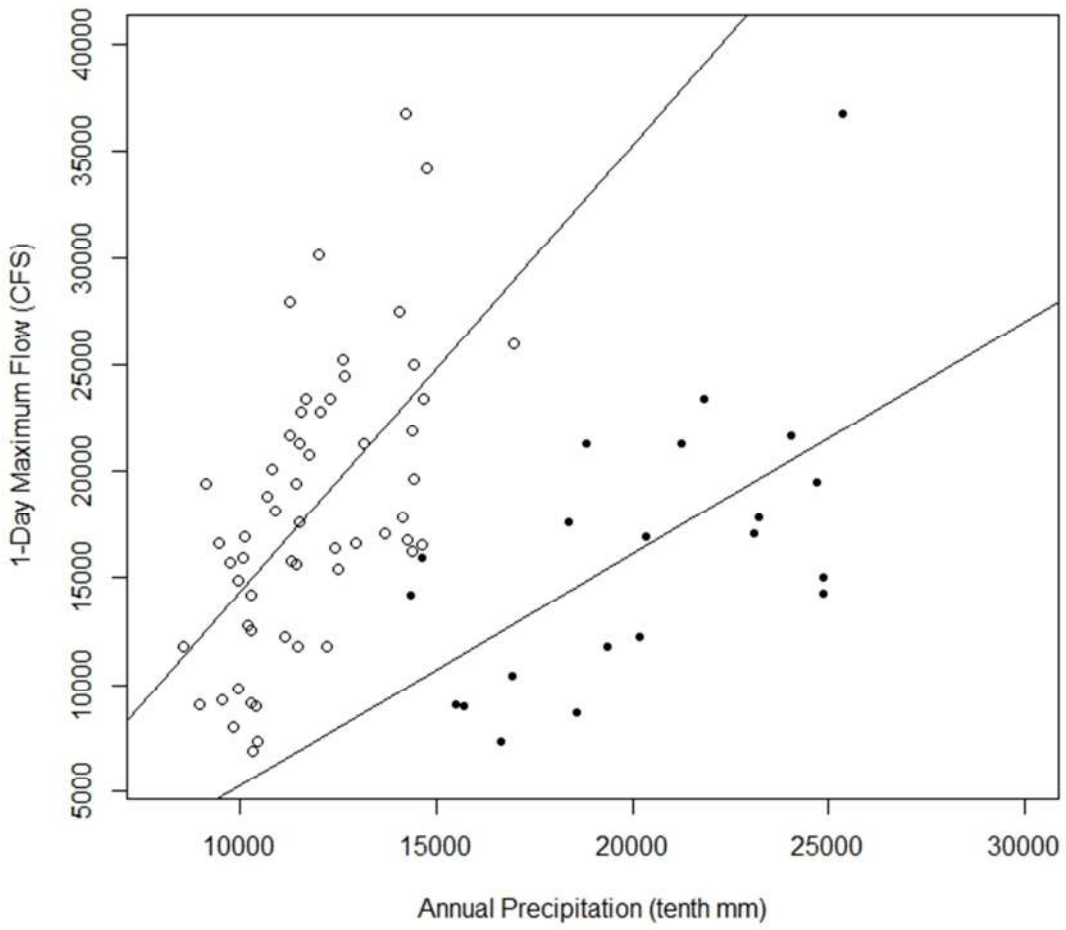

Figure 12: Cumulative annual precipitation at Arlington, WA (open circles) and Darrington, WA (solid circles) and days above 7-day median high flow with linear regression trend lines.

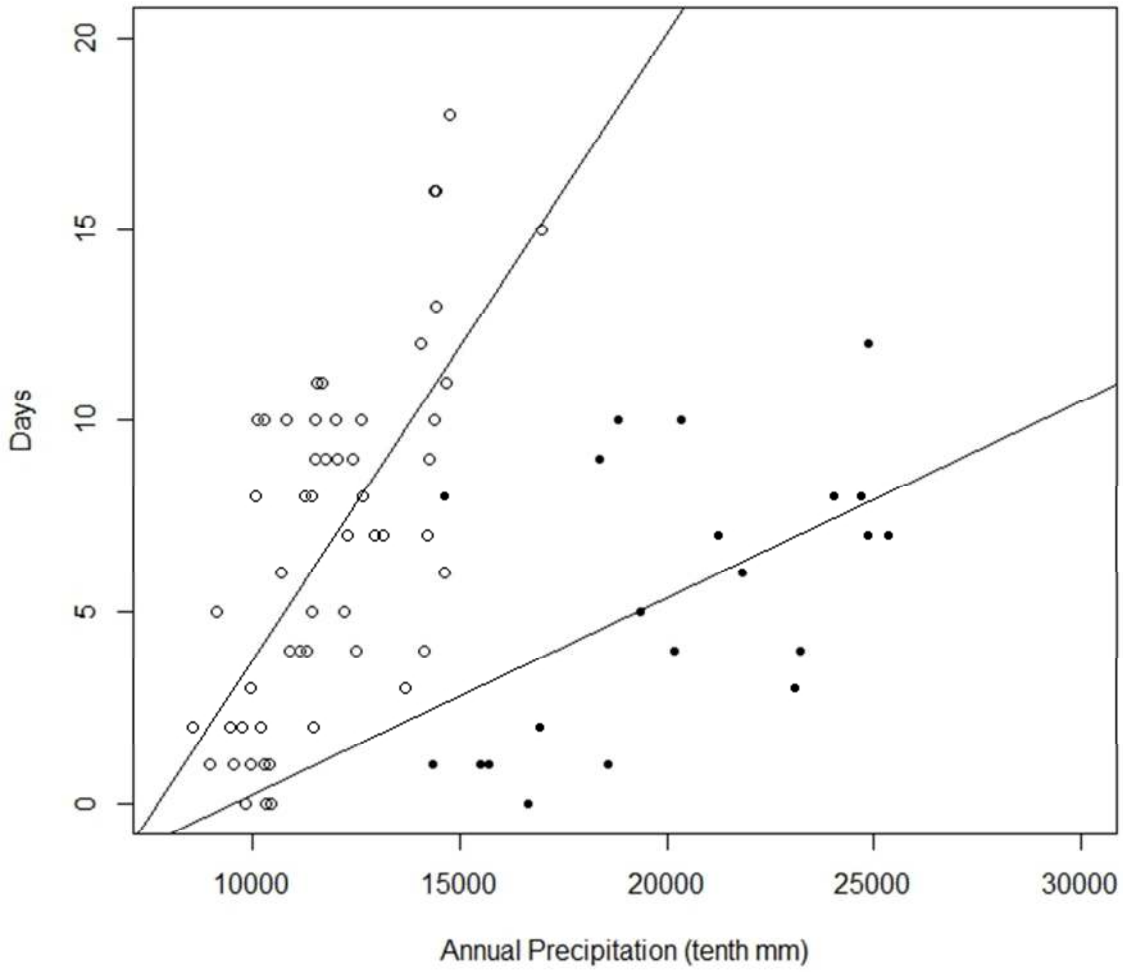

Figure 13: Cumulative annual snowfall at Darrington, WA and 90-day minimum flow with linear regression trend lines.

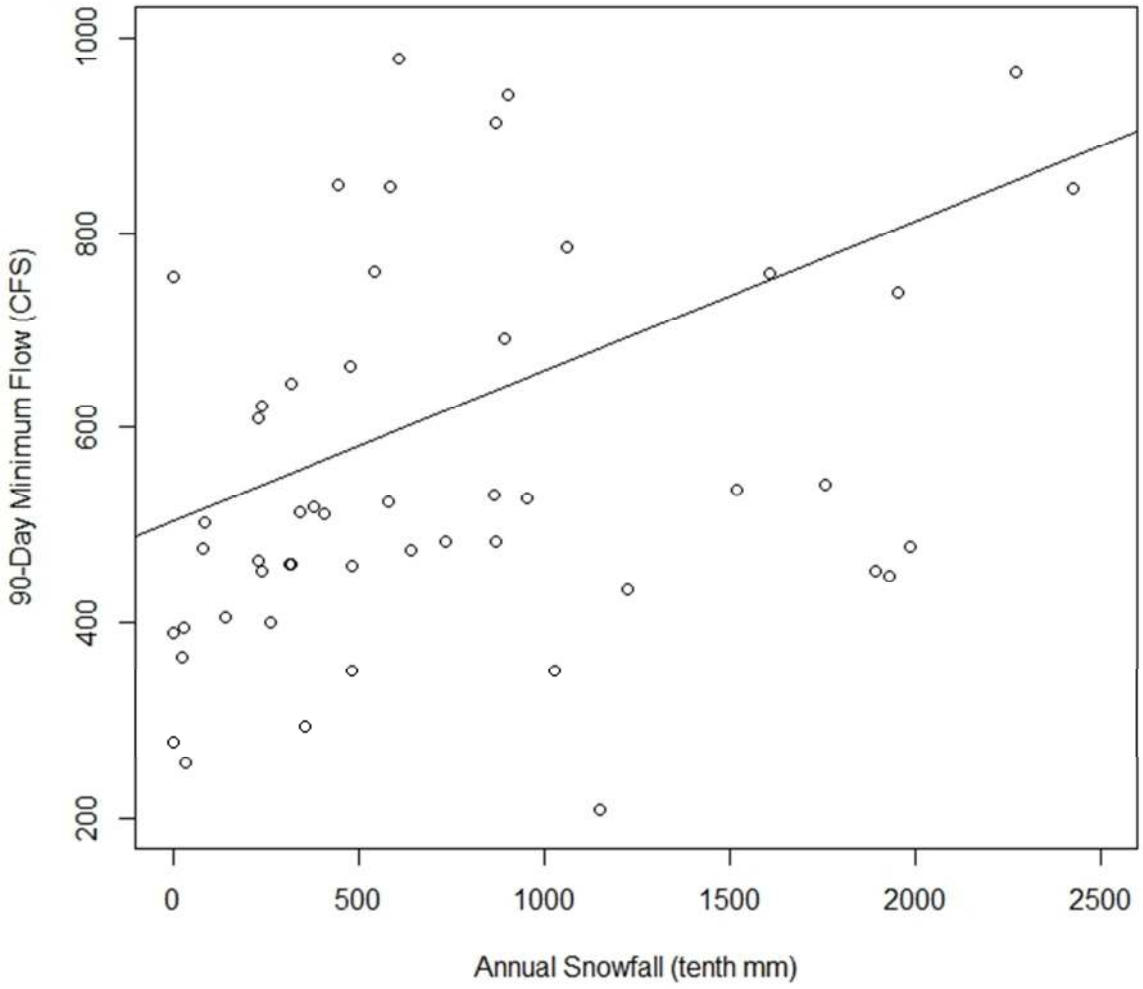

Figure 14: Proportion immature land cover and 1-day minimum flows (open circle) and 90-day minimum flows (closed circle) with linear regression fit.

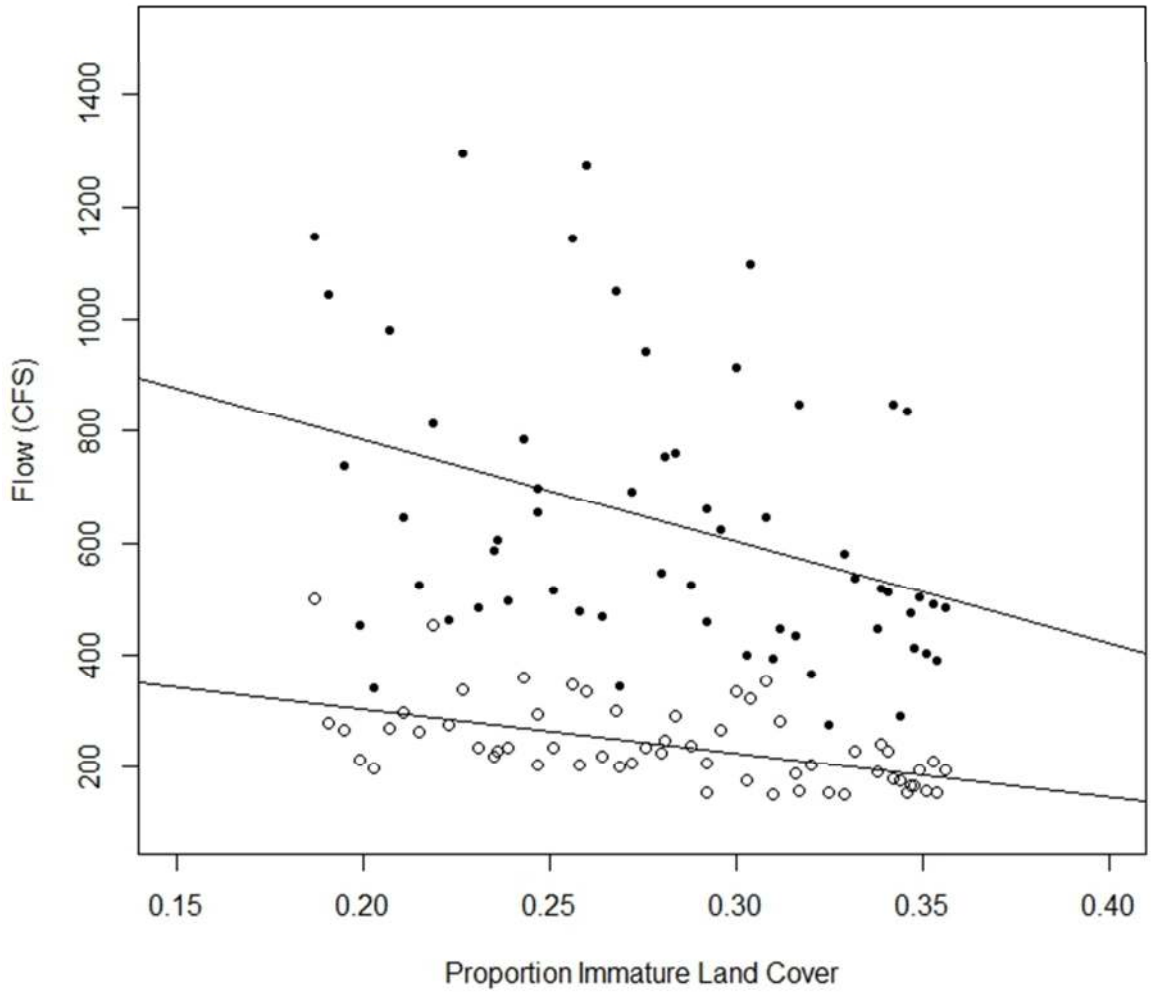

Figure 15: Proportion immature land cover and 1-day maximum flows with linear regression fit.

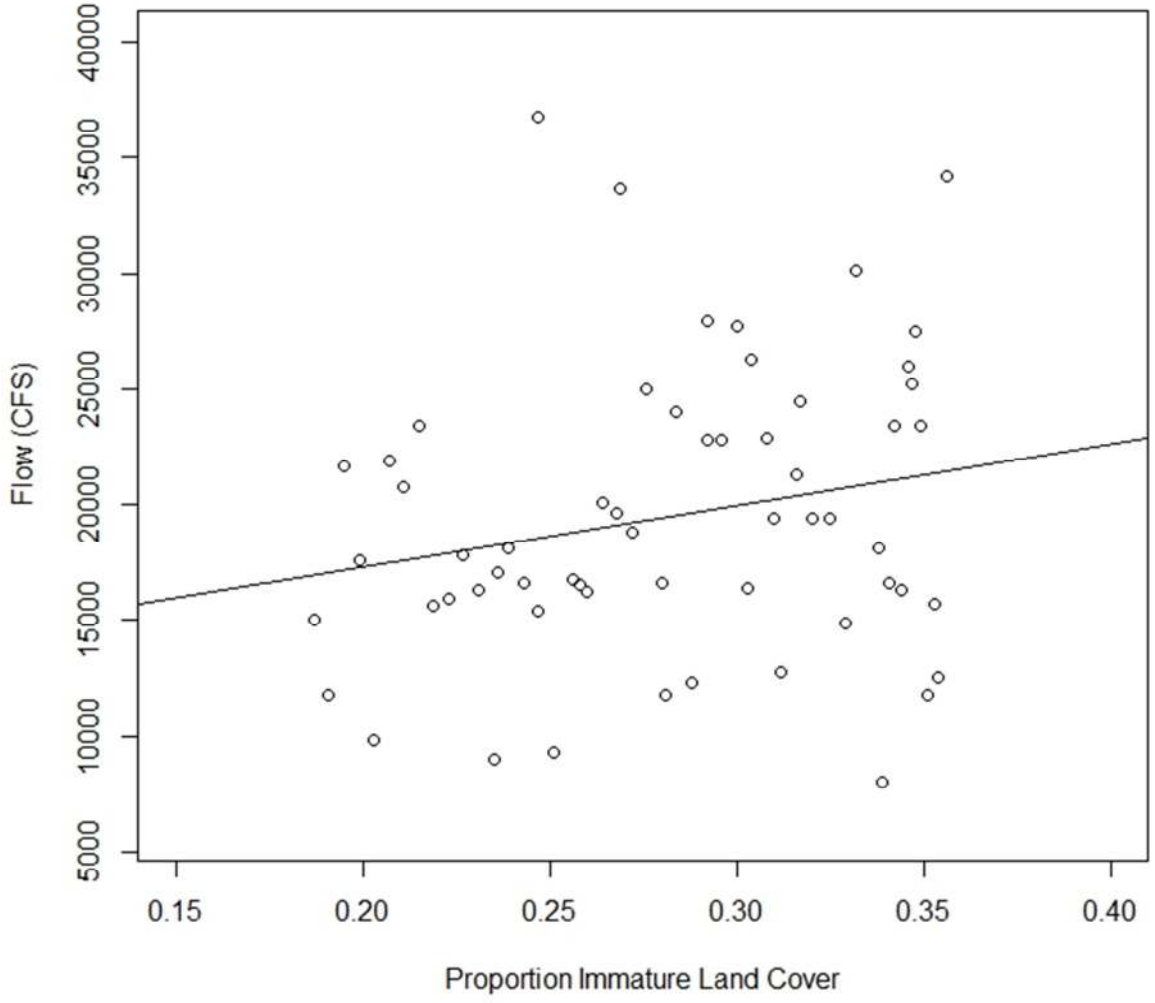

Figure 16: Observed 1-day max flow (black solid line) by water year with predicted 1-day maximum flows (red solid line) and the lower and upper 95% confidence intervals for the predicted 1-day maximum flows (dashed lines). Prediction gaps are the result of local climate data gaps for some water years.

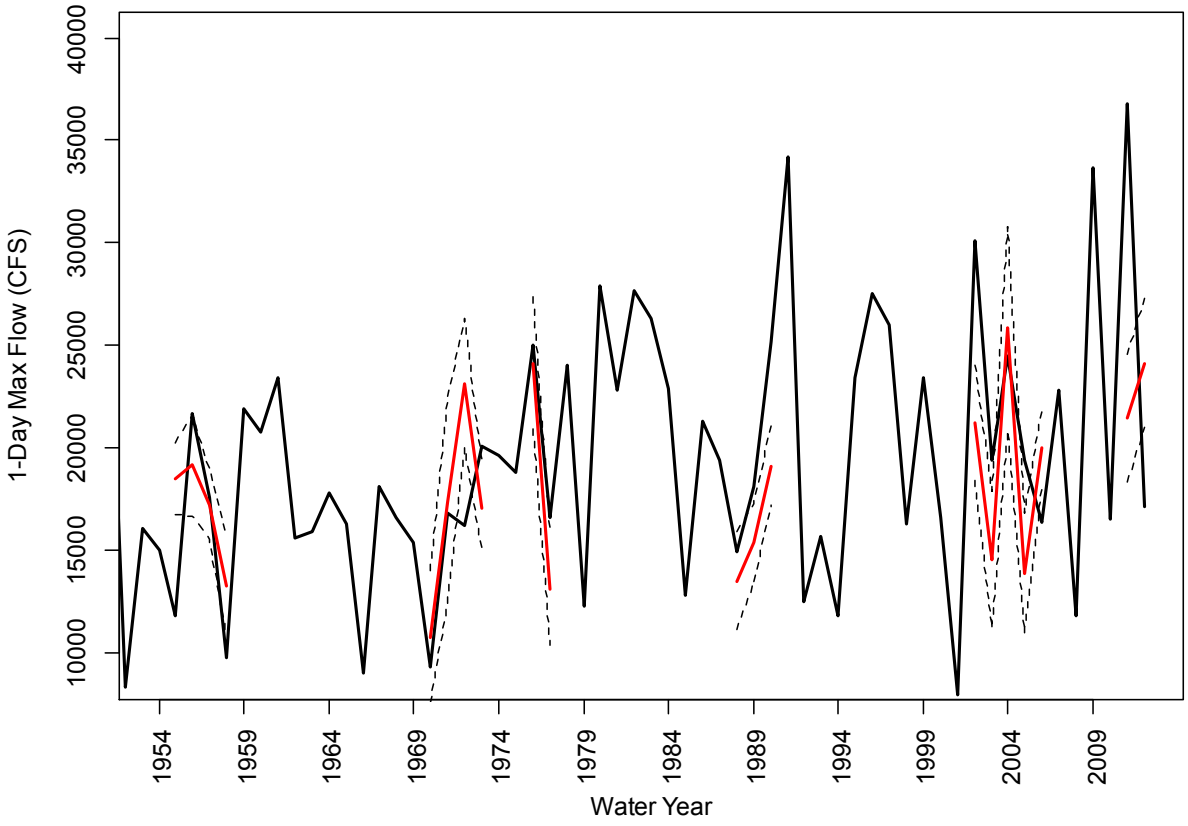

Figure 17: Observed 1-day minimum flow (black solid line) by water year with predicted 1-day minimum flows (red solid line) and the lower and upper 95% confidence intervals for the predicted 1-day minimum flows (dashed lines).

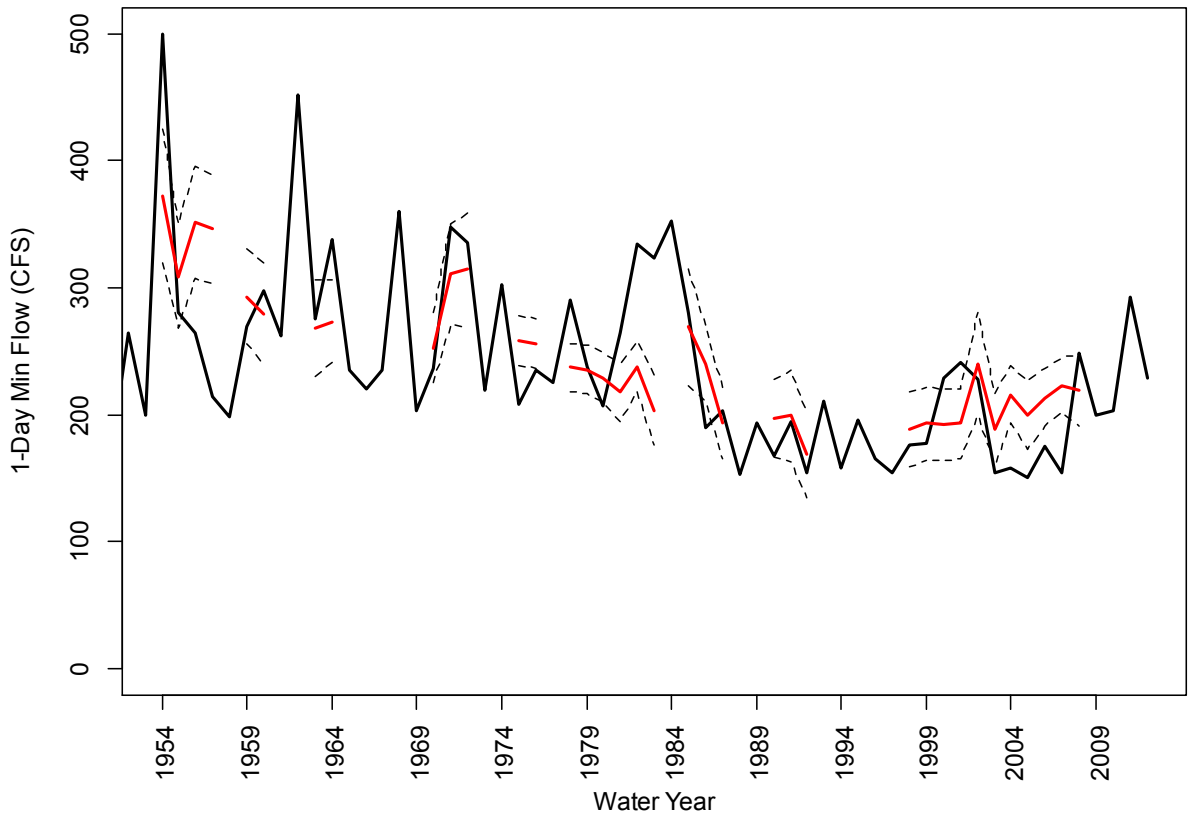

Appendix A: Measured (bold values) and predicted proportion immature and mature land cover by year from linear regressions between measured years.

Water Year	Proportion Immature	Proportion Mature	Water Year	Proportion Immature	Proportion Mature
1954	**0.187**	**0.813**	1984	0.308	0.692
1955	0.191	0.809	1985	0.312	0.688
1956	0.195	0.805	1986	0.316	0.684
1957	0.199	0.801	**1987**	**0.320**	**0.680**
1958	0.203	0.797	1988	0.329	0.671
1959	0.207	0.793	1989	0.338	0.662
1960	0.211	0.789	1990	0.347	0.653
1961	0.215	0.785	**1991**	**0.356**	**0.644**
1962	0.219	0.781	1992	0.354	0.646
1963	0.223	0.777	1993	0.353	0.647
1964	0.227	0.773	1994	0.351	0.649
1965	0.231	0.769	1995	0.349	0.651
1966	0.235	0.765	1996	0.348	0.653
1967	0.239	0.761	1997	0.346	0.654
1968	0.243	0.757	1998	0.344	0.656
1969	0.247	0.753	1999	0.342	0.658
1970	0.251	0.749	2000	0.341	0.659
1971	0.256	0.744	**2001**	**0.339**	**0.661**
1972	0.260	0.740	2002	0.332	0.668
1973	0.264	0.736	2003	0.325	0.675
1974	0.268	0.732	2004	0.317	0.683
1975	0.272	0.728	2005	0.310	0.690
1976	0.276	0.724	**2006**	**0.303**	**0.697**
1977	0.280	0.720	2007	0.292	0.708
1978	0.284	0.716	2008	0.281	0.719
1979	0.288	0.712	2009	0.269	0.731
1980	0.292	0.708	2010	0.258	0.742
1981	0.296	0.704	**2011**	**0.247**	**0.753**
1982	0.300	0.700	2012	0.236	0.764
1983	0.304	0.696			